Available online at www.sciencedirect.com

ScienceDirect

Genomics 89 (2007) 207–214

GENOMICS

www.elsevier.com/locate/ygeno

A series of ENU-induced single-base substitutions in a long-range *cis*-element altering Sonic hedgehog expression in the developing mouse limb bud

Hiroshi Masuya [a], Hideki Sezutsu [b], Yoshiyuki Sakuraba [b], Tomoko Sagai [c], Masaki Hosoya [c], Hideki Kaneda [a], Ikuo Miura [a], Kimio Kobayashi [a], Kenta Sumiyama [d], Aya Shimizu [a], Junko Nagano [a], Haruka Yokoyama [a], Satoko Kaneko [b], Noriko Sakurai [c], Yuka Okagaki [c], Tetsuo Noda [a], Shigeharu Wakana [a], Yoichi Gondo [b], Toshihiko Shiroishi [a,c,*]

[a] *Mouse Functional Genomics Research Group, RIKEN GSC 3-1-1 Kouyadai, Tsukuba, Ibaraki 305-0074, Japan*
[b] *Population and Quantitative Genomics Team, RIKEN GSC 1-7-22 Suehiro-cho, Tsurumi-ku, Yokohama City, Kanagawa 230-0045, Japan*
[c] *Mammalian Genetics Laboratory, National Institute of Genetics, Yata 1111 Mishima, Shizuoka-ken 411-8540, Japan*
[d] *Division of Population Genetics, National Institute of Genetics, Yata 1111 Mishima, Shizuoka-ken 411-8540, Japan*

Received 29 June 2006; accepted 15 September 2006
Available online 13 October 2006

Abstract

Mammal–fish-conserved-sequence 1 (MFCS1) is a highly conserved sequence that acts as a limb-specific *cis*-acting regulator of Sonic hedgehog (*Shh*) expression, residing 1 Mb away from the *Shh* coding sequence in mouse. Using gene-driven screening of an ENU-mutagenized mouse archive, we obtained mice with three new point mutations in MFCS1: *M101116*, *M101117*, and *M101192*. Phenotype analysis revealed that *M101116* mice exhibit preaxial polydactyly and ectopic *Shh* expression at the anterior margin of the limb buds like a previously identified mutant, *M100081*. In contrast, *M101117* and *M101192* show no marked abnormalities in limb morphology. Furthermore, transgenic analysis revealed that the *M101116* and *M100081* sequences drive ectopic reporter gene expression at the anterior margin of the limb bud, in addition to the normal posterior expression. Such ectopic expression was not observed in the embryos carrying a reporter transgene driven by *M101117*. These results suggest that *M101116* and *M100081* affect the negative regulatory activity of MFCS1, which suppresses anterior *Shh* expression in developing limb buds. Thus, this study shows that gene-driven screening for ENU-induced mutations is an effective approach for exploring the function of conserved, noncoding sequences and potential *cis*-regulatory elements.

Keywords: *cis*-regulatory element; MFCS1; Sonic hedgehog; Noncoding sequence; ENU; Mutagenesis; Single nucleotide polymorphism; Limb development; Axis formation

Control of polarity is essential for establishing the vertebrate body plan. Sonic hedgehog (Shh) is a secreted signaling protein involved in establishing polarity in many developing tissues [1–4], whose expression is tightly regulated and restricted to specific spatiotemporal patterns during organogenesis. In vertebrate limb morphogenesis, patterning along the antero-posterior (A-P) axis is controlled by the zone of polarizing activity (ZPA) at the posterior margin of the limb bud [5,6]. *Shh* is expressed exclusively in the mesenchyme of the ZPA and establishes A-P polarity in the distal limb bud [7–15] The expression pattern of *Shh* in the posterior limb bud is affected in many mouse mutants, including the *Xt*, *lst*, *Rim4*, *lx*, *Xpl*, *Dh*, and *Hx*, all of which exhibit preaxial polydactyly (PPD). In these mutants, ectopic *Shh* expression is observed at the anterior margin of the limb bud, resulting in double posterior autopods [16–22]. In addition, analysis of two PPD mutants, *XtJ* and *lstJ*, which have loss-of-function mutations in *Gli3*

* Corresponding author. Fax: +81 29 836 9017.
E-mail address: tshirois@lab.nig.ac.jp (T. Shiroishi).

0888-7543/$ - see front matter © 2006 Elsevier Inc. All rights reserved.
doi:10.1016/j.ygeno.2006.09.005

and *Alx4*, suggests that there is a negative regulatory mechanism controlling *Shh* expression at the anterior margin of the limb bud [18,19].

Recently, others and we reported that a limb-specific, long-range *cis*-acting regulator controls *Shh* transcription in the posterior margin of the limb bud. This 1-kb sequence is located in intron 5 of the *Lmbr1* gene, approximately 1 Mb away from the *Shh* coding region [23–26]. Its action is independent of other short-range *cis*-regulatory elements that regulate *Shh* expression in the notochord or neural tube [27]. As this sequence is highly conserved between mammals and fish, we have referred to it as mammal–fish-conserved-sequence 1 (MFCS1). Interestingly, in limbless vertebrates such as the snake, limbless lizard, and newt, MFCS1 sequences were not detected by Southern blot analysis [26], suggesting that this sequence is not required in limbless species.

Mutational analysis of MFCS1 has yielded some insights into its function. Deletion of a 1.2-kb fragment including MFCS1 by gene targeting in mice causes loss of *Shh* expression only in the developing limb buds, as well as defects in formation of distal skeletal elements of all four limbs [28]. A similar phenotype was observed in the spontaneous chick mutant oligozeugodactyly (*ozd*), which lacks *Shh* function in the limb [29,30]. In addition, MFCS1 drives transgenic reporter gene expression specifically in the posterior fore-and hind-limb buds in mice, indicating that MFCS1 contains a limb-specific enhancer [25,26,28]. Together, these studies demonstrate that MFCS1 positively regulates *Shh* expression in the posterior limb bud.

However, single-base substitutions in MFCS1 in the *Hx* and *M100081* alleles result in a PPD phenotype, which is typically associated with ectopic expression of *Shh* in the anterior of the limb bud [25,26]. In addition, a transgenic assay showed that a MFCS1 sequence harboring an *Hx*-type mutation drives ectopic reporter gene expression in the anterior margin of the limb bud [31]. Moreover, in humans, several family cases of PPD exhibited point mutations in the core region of MFCS1 [25]. These data suggest that MFCS1 is also involved in the negative regulation of *Shh* in the anterior margin of the limb bud, and its defect causes PPD [31].

As no known molecular motifs have been found in the MFCS1 sequence, additional mouse mutants with single-base substitutions at different sites in MFCS1 would be invaluable for testing out the molecular mechanism of *cis*-regulation by MFCS1. *N*-Ethyl-*N*-nitrosourea (ENU) is a highly potent chemical mutagen, which induces multiple single-base-pair changes randomly on genomic DNA at very high efficiency [32–36]. Several large-scale mouse ENU mutagenesis projects have been conducted in many countries [37–44] and have demonstrated that genetic analysis using multiple ENU-induced mutant alleles is a powerful approach for dissecting the function of a given domain of an individual gene [45–49].

We have established a highly efficient gene-driven screening system for ENU-induced mutations using temperature-gradient capillary electrophoresis (TGCE), which enables high-throughput detection of heteroduplexes of normal and mutated genomic DNA fragments with single base substitutions following PCR amplification of target genes [36,50,51]. In this study, we have used this system to screen for single-base substitutions in MFCS1 and obtained three new mutations. We report the results of phenotype characterization of these three mutant mice and transgenesis analysis using a reporter gene flanked by DNA sequences of the three MFCS1 mutants.

Results

Gene-driven screening of mutations in MFCS1

To explore the function of MFCS1, we screened a genomic DNA archive of our ENU-mutagenized mice. Using the VISTA alignment tool (http://gsd.lbl.gov/vista/), we identified a region of MFCS1 that is highly conserved between mouse, human, chick, and fugu (Fig. 1). We were able to amplify two different fragments with two sets of PCR primers (A and B), which cover a 994-bp segment (position 17 to 1011) of the mouse–chick conserved region of MFCS1. When genomic DNA was amplified from G1 founder animals heterozygous for the ENU-induced mutation in MFCS1, the PCR products formed a heteroduplex resulting from the single-base mismatch pair, which was easily detected by TGCE analysis. We screened 3416 G1 individuals using primer pair A and 3980 using primer pair B (Table 1). Three new mutants with single-base substitutions at different sites in the targeted region were identified: *M101116* (A to G at position 204), *M101117* (A to G at position 409), and *M101192* (A to T at position 800).

In the VISTA alignment, position 204, which was mutated in *M101116*, was conserved in all four species examined (mouse, human, chick, and fugu). The bases that were mutated in *M101192* and *M101117* were conserved in mouse, human, and chick (Table 2). The substitution sites of these three mutations in MFCS1 are overlaid on the sites of previously reported mouse and human PPD mutations in Fig. 1 [25,26].

Limb phenotype of the three new mutations in the highly conserved region of MFCS1

The original G^1 heterozygous founder animals of the three mutant lines showed no marked anomalies in adult limb morphology. We backcrossed these animals to wild-type C57BL/6J mice to generate G^2 heterozygous progeny and then intercrossed these heterozygotes to obtain homozygous G^3 progeny. We also examined the gross phenotype of the preexisting ENU-induced PPD mutant *M100081* [26], with particular attention to the dermal ridge pattern [52]. We found that *M101117* and *M101192* exhibited no limb morphology defects, either in heterozygous or in homozygous animals. On the other hand, *M101116* and *M100081* had a clear semidominant PPD phenotype: 26.6% of *M101116* G^2 heterozygotes and 80% of G^3 heterozygotes exhibited the PPD phenotype. This difference might be due to differences in genetic background. G^3 homozygotes of *M101116* showed full (100%) penetrance of the PPD phenotype. These mating experiments also indicated linkage of *M101116* and PPD phenotype. Tibial hemimelia, which is a severe form of PPD, was not detected in G^2 or G^3 *M101116* heterozygotes or homozygotes. The penetrance of the

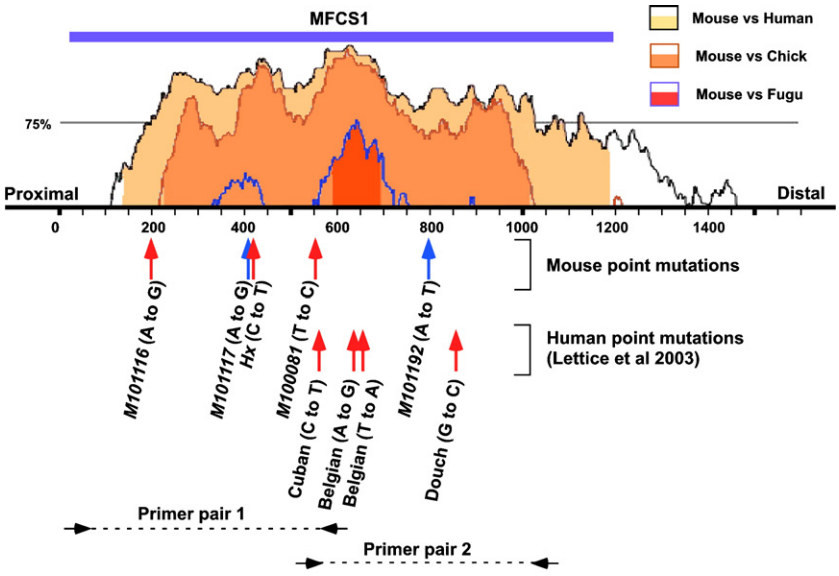

Fig. 1. Locations of point mutations in MFCS1. Nucleotide substitution sites of newly obtained and preexisting point mutations in mouse and human are superimposed on the MFCS1 sequence. In the VISTA analysis, we used a 100-bp window length and 70% conservation level for mouse–human, mouse–chick, and mouse–fugu comparisons. The MFCS1 region [26] is represented by a blue horizontal line above the VISTA graphs. Blue arrows indicate no phenotype in limb morphology, red arrows indicate locations of PPD mutation of mouse and human. Locations of the primer pairs used in TGCE analysis (Table 1) are represented by black horizontal arrows.

PPD phenotype in *M100081* heterozygotes was 97.5% for G^2 and 100% for G^3 animals. All *M100081* homozygotes displayed the more severe form of PPD, tibial hemimelia, in both G^2 and G^3 animals.

Point mutations in MFCS1 caused ectopic expression of Shh at the anterior margin of the limb bud

The adult skeletons of *M100081* and *M101116* mutants exhibited tripharangeal digit 1 or extra digits, which indicate a mirror-image duplication (Figs. 2A to 2C). To determine whether the mutations in MFCS1 affect regulation of *Shh*, we examined *Shh* expression in the limb bud of E10.5 *M100081* and *M101116* embryos by whole-mount *in situ* hybridization. At stage 5 of mouse limb development [53], ectopic *Shh* expression was detected in all three homozygous *M100081* embryos (Fig. 2E) and four of six homozygous *M101116* embryos (Fig. 2F) analyzed. The ectopic anterior expression of *Shh* was clearly weaker in *M1001116* embryos than in *M100081* embryos.

Next, we generated transgenic embryos that have the β-gal reporter gene flanked by 1.2-kb fragments of the mutant MFCS1 sequences, *M10116*, *M101117*, and *M100081* (Fig. 3A). *M101116* and *M100081* transgenic embryos showed significant levels of ectopic reporter gene expression at E10.5 and E11.5 at the anterior margin of all limb buds, in addition to the normal posterior margin expression. In contrast, no ectopic expression was detected in transgenic embryos with the *M101117* MFCS1 fragment (Table 3 and Fig. 3).

Discussion

Efficacy of gene-driven screening for ENU-induced mutations in MFCS1

Cross-species comparison of genomic DNA sequence is an important method for identifying biologically important genomic elements. This approach often aids in the identification of functional *cis*-regulatory elements. To examine the function of MFCS1, a *cis*-regulatory element for *Shh*, we employed a large-scale gene-driven screen of ENU-induced mutations, using TGCE to perform high-throughput mutation analysis [36] by automatic heteroduplex detection [50,51]. We screened the targeted MFCS1 sequences of about 3500 individuals from our mutant mice archive, amounting to a total of approximately 3.8 Mb of sequence examined. From this screen, we obtained three new mutations, *M101116*, *M101117*, and *M101192*.

These mutants with single-base-pair substitutions exhibited different levels of ectopic *Shh* expression. Although such substitutions are not generally regarded as a major cause of functional defects in *cis*-regulatory elements, many studies

Table 1
Summary of results of gene-driven screening of MFCS1

Primer pair	Primer 1	Primer 2	Product length (position)	No. screened	Length screened (bp)	Mutants detected	Mutation ratio (detected)
Pair A	CCAGATGACTTTTCCCCTCA	AGTTCAAGAAACCGCACACC	538 (17 to 554)	3416	1,837,808	2	1.1×10^{-6}
Pair B	ggcgcAGCCCAGGACTTTTTCTGGT [a]	AAGATGGAGGCCTGAGACAA	506 (506 to 1011)	3980	2,013,880	1	5.0×10^{-7}
Total					3,851,688	3	7.8×10^{-7}

[a] The "ggcgc" sequence is a GC clamp.

Table 2
Position, phenotype and its penetrance of mutations in MFCS1

Mutant	Mouse MFCS1 position	Mutation	Conservation [a]	Category	Phenotype of founder	Heterozygous phenotype	Heterozygous penetrance	Homozygous phenotype	Homozygous penetrance
M101116	204	ATTAACACAT<A to G>GCAACAGTTAG	4 species	ENU induced	Normal	Polydactyly	26.6% (4/15) 80% (4/5) [b]	Polydactyly	100% (4/4)
M101117	409	CCAACAATTT<A to G>TGGATCATCA	3 species	ENU induced	Normal	Normal	0% (0/20)	Normal	0% (0/6)
Hx	418	TATGGATCAT<C to T>AGTGGCAAAA	4 species	Natural mutation	(Hemimelia, polydactyly)	Hemimelia, polydactyly	100%	Hemimelia, polydactyly	100%
M100081	563	GGTCATAAAA<T to C>ACAGTACAAG	4 species	ENU induced	Polydactyly	Polydactyly	97.1% (34/35)	Hemimelia, polydactyly	100% (14/14)
M101192	800	TACTTTTATT<A to T>TGAAAGTACT	3 species	ENU induced	Normal	Normal	0% (0/33)	Normal	0% (0/13)

[a] Conservation among human, mouse, chick, and fugu sequences.
[b] Penetrance differed according to generation (26.6% in G2 and 80% in G3).

investigating the mechanisms of transcriptional regulation indicate that single-base substitutions can cause gross changes in binding affinity of *cis*-elements to *trans* factors and thus result in changes in gene expression level. For example, altered gene expression level by single-base-pair substitution has been demonstrated for the butyrate response element [54], the hepatitis B virus enhancer II B1 element [55], and NF-1 binding elements [56]. In addition, expression quantitative trait locus (QTL) analysis performed by crossing different mouse strains often reveals QTLs mapped near coding regions [57–59]. Such *cis*-acting QTLs may result from single-nucleotide polymorphisms (SNPs) in *cis*-regulatory regions. In addition, in humans, SNPs are associated with changes in gene expression in diseases such as breast cancer and osteoarthritis [60,61].

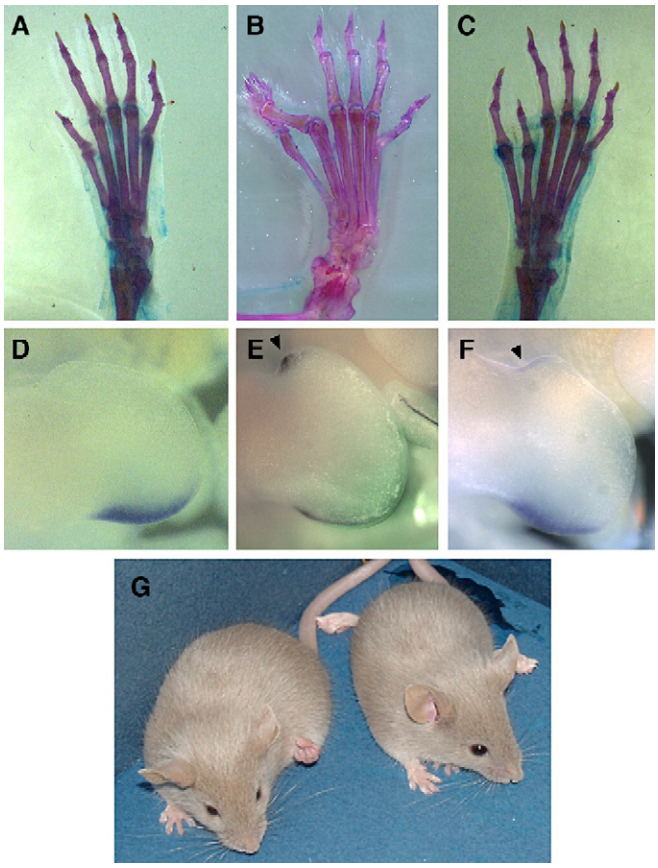

Fig. 2. Skeletal and molecular phenotype in *M100081* and *M101116*. Alizarin red and Alcian blue staining of limb skeletons of (A) wild-type, (B) *M100081* homozygous, and (C) *M101116* homozygous animals, showing PPD phenotype in *M100081* and *M101116* homozygotes. (D–F) Expression of *Shh* in hind-limb bud at E10.5 by whole-mount in situ hybridization. Ectopic *Shh* expression at the anterior margin of the limb bud was detected in (E) *M100081* and (F) *M101116* homozygotes. Arrowheads indicate ectopic *Shh* expression. (G) *M100081* homozygotes showed hemimelic tibia, a serious form of PPD.

Based on the present analysis, the mutation rate per base pair was calculated to be 7.8×10^{-7}, a figure that is consistent with our previous estimate (7.84×10^{-7}) based on data from earlier identified mutants (155 point mutations from a screen of 197 Mb total target sequence) [36]. This suggests that TGCE screening of ENU-treated animals is one of the most efficient methods of obtaining mutations in *cis*-elements as well as coding sequences, especially compared to other genetic engineering techniques, such as knock-in approaches. Altogether, our study demonstrates that gene-driven screening of ENU-mutagenized mouse archives is an efficient way to identify mice with single-base-pair substitutions in *cis*-regulatory elements.

Negative regulatory activity of MFCS1 was disrupted by broadly distributed nucleotide substitutions

Deletion of MFCS1 abolishes *Shh* expression in the developing limb bud [28], whereas a point mutation in MFCS1, *Hx*, causes a PPD phenotype that appears to result from ectopic *Shh* expression in the anterior mesenchyme of the limb bud [25,26,30]. In this study, we analyzed newly obtained and preexisting mutations in the highly conserved core sequence of MFCS1. Two mutations, *M101116* and *M100081*, showed double posterior PPD phenotypes with ectopic expression of *Shh* at the anterior margin of the limb bud. Transgenic analysis confirmed that *M101116* and *M100081* sequences induced ectopic *Shh* expression, as did the *Hx* mutation [30]. These data suggest that negative regulation of

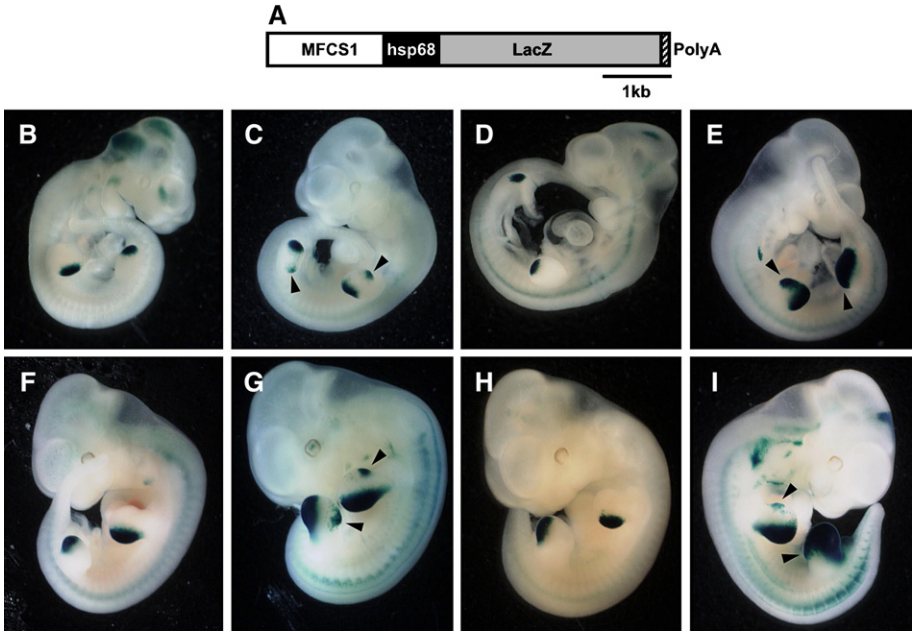

Fig. 3. Enhancer activity of the MFCS1 mutations using transgenic analysis. (A) Basic structure of transgenic constructs. Wild-type or mutant MFCS1 fragments (white) were placed adjacent to the hsp68 promoter (solid) and *LacZ* reporter gene (shaded). A SV40 polyadenylation signal is represented by the striped box. Transgenic mouse embryos were stained with X-gal at (B–E) E10.5 and (F–I) E11.5. Wild-type embryos showed localized β-gal in the posterior region of the limb bud (B and F), whereas ectopic β-gal activity was detected in all transgenic embryos carrying *M101116* (C and G) and *M100081* (E and I) mutations at E10.5 and E11.5. In contrast, all transgenic *M101117* embryos (D and H) showed normal β-gal expression. Arrowheads indicate ectopic expression of the reporter gene at the anterior margin of limb buds.

Shh expression is easily disrupted by single-nucleotide changes at multiple sites broadly distributed along the MFCS1 sequence. On the other hand, these mutants affected the negative regulation by MFCS1 to different degrees. For instance, *M101116* mutants exhibited a mild PPD phenotype, *M100081* mutants had an intermediate phenotype, and *Hx* mutants had the severest phenotype (Table 2) [26]. In contrast, *M101192* and *M101117* mutants showed no defects in limb development. Degree of the phenotypes of the mutants coincided with the level of ectopic *Shh* expression in the respective mutants. In addition, ectopic *Shh* expression in *M101116* mutants may depend on developmental stage, since we were able to detect ectopic expression only at stage 5 in E10.5 embryos (data not shown), although it was hard to show reproducible correlation between the levels of *LacZ* reporter expression at the anterior mesenchyme of the limb buds in the transgenic mice and the level of the ectopic *Shh* expression in the respective mutants. We observed no ectopic *Shh* or LacZ expression in *M101117* embryos. This mutation seems to be completely “silent” for the limb phenotype. It is unclear at present why this site has been conserved so long, beyond speciation of a common ancestor into mouse, human, and chick.

Table 3
Frequency of ectopic expression in the anterior margin of the limb bud in transgenic analysis of MFCS1

Genotype of MFCS1 mutation	Ectopic/assayed (normal)		
	10.5 dpc	11.5 dpc	Total
M100081	6/6	4/4	10/10
M101116	5/5	2/2	7/7
M101117	0/3	0/6	0/9

We aligned four human MFCS1 mutations associated with PPD [25] and the three mouse mutations in the MFCS1 sequence (Fig. 1). We found no domain-like structure in which the mutations are clustered. In fact, the mutation site of *Hx*, which produces the most severe PPD phenotype, was just adjacent to that of *M101117*, which has normal limb morphology. It is of interest to note that the degree of the PPD phenotype tends to correlate with conservation of nucleotide at the mutation sites. As summarized in Table 2, polydactylous mutations, *Hx*, *M100081*, and *M101116*, have substitutions at the conserved nucleotides among four species, human, mouse, chick, and fugu. In contrast, nonpolydactylous mutations, *M101117* and *M101192*, have substitutions at the nucleotides conserved in three species, human, mouse, and chick. These two nucleotides are deleted in the aligned fugu sequence (data not shown). It was reported that the fugu MFCS1 could drive posterior expression of a reporter gene in developing mouse limb buds [25]. Thus, it seems possible there may be common mechanism of polarized *Shh* expression in developing fin buds of fishes and in limb buds of tetrapod organisms, which requires the MFCS1 sequence. It was also reported that two of four polydactylous substitutions in human are conserved in the above four species including fugu [25], but the remaining two sites are not conserved in the fugu genome, suggesting some minor difference in fishes and tetrapods in the negative regulation that involves MFCS1.

Notably, none of the three MFCS1 mutations *Hx*, *M100081*, and *M101116* disrupted the positive regulation of *Shh*

expression at the posterior of the limb bud. In transgenic assay a partial fragment of MFCS1 that deletes a region including the nucleotide site that is mutated in *Hx* leads to reduced expression levels of the reporter gene at the posterior limb buds, but this fragment did not induce ectopic expression of the reporter gene at the anterior region of the limb buds [25]. Thus, it is possible that ectopic *Shh* expression may require flanking sequence surrounding the mutation sites. It is likely that the single base substitutions in MFCS1 induce erroneous binding of some transacting factor(s), which results in upregulation of *Shh* at the anterior margin of the limb bud. It is known that positive regulation in the posterior region of the limb bud involves the basic helix–loop–helix transcription factor dHand [62,63] and that expression of *dHand* is not altered in *Hx* homozygotes [26]. Another transcription factor, eHand, has biochemical activity similar to that of dHand and is expressed in the anterior region of limb buds [64]. It is possible that the MFCS1 mutations may provoke erroneous binding to an unknown transacting factor(s) and it may interact with eHand to promote ectopic expression of *Shh* at the anterior margin of limb buds.

Materials and methods

Mouse ENU mutagenesis

C57BL/6J and DBA/2J mice were purchased from CLEA Japan, Inc. (Tokyo, Japan). The G1 founder animals heterozygous for ENU-induced mutations were produced by crossing DBA/2J females to C57BL/6J males that were administered 150–250 mg/kg ENU. Detailed protocols for ENU mutagenesis can be found at the Web site http://www.gsc.riken.go.jp/Mouse/, as previously reported [45]. Basic phenotype screening of G1 founder animals was performed using the modified SHIRPA method [44]. Sperm samples from all of the male founders were cryopreserved in liquid nitrogen, and gonads were collected at the same time to obtain genomic DNA [36].

Gene-driven screening for mutations in MFCS1

Gene-driven screening using TGCE analysis was carried out as previously described [36]. The system is able to detect conformation changes in double-stranded DNA containing base-pair mismatches [51]. Primer pairs used for PCR amplification and TGCE analysis are summarized in Table 1. Information on the three point mutations in the core region of MFCS1 as well as other three-point mutations that occurred in the less conserved region of MFCS1 is posted on our Web site, and the mutants are available for distribution (http://www.gsc.riken.jp/Mouse/).

Comparison of genomic DNA sequences

The cross-species comparison of the MFCS1 sequence among mouse, human, chick, and fugu was performed using the VISTA program (http://gsd.lbl.gov/vista/). Genomic sequences were obtained by a BLAST search (http://www.ensembl.org/), using the highly conserved sequence (TCTATCCTGTGT-CAGTTTGA) reported previously [25,29].

Genotyping animals

Following gene-driven screening, G^1 founder animals were crossed to wild-type animals to assess penetrance of the phenotype. The G^2 progeny were genotyped by direct sequencing of the amplified products using primer pair A (Table 1) for detecting the *M101116* and *M101117* mutations and primer pair B (Table 1) for detecting the *M101192* mutation.

In situ hybridization

Whole-mount in situ hybridization using digoxigenin-labeled RNA was performed as described elsewhere [17]. The probe for *Shh* was transcribed from a 642-bp *Eco*RI fragment using T3 polymerase [1].

Transgenic analysis

Fragments of MFCS1 (1.2 kb) were amplified from genomic DNA from homozygous *M101116*, *M101117*, and *M100081* and wild-type animals by PCR using primers reported elsewhere [29]. These fragments were subcloned into the HSF51 vector with the mouse hsp68 basic promoter and the bacterial *LacZ* coding region [65,66]. Standard pronuclear injection technique was used to generate transgenic animals with these constructs [3]. G^0 embryos were harvested at E10.5 or E11.5 and stained for β-gal activity, as previously described [30]. Genotyping of transgenic embryos was performed using PCR with primers TCACCCTGCCATAAAGAAACT and CTGTCGTCGTCCCCTCAAACT to detect integrated vector sequence.

Acknowledgments

We thank Drs. Masaru Tamura, Takanori Amano, and Takuya Murata for helpful discussions. We also thank the technical staffs of the Functional Genomics Research Group of RIKEN GSC for gene-driven screening, animal care, and phenotype screening. This study was supported in part by the National Bioresources Project and Grants-in-Aid from the Ministry of Education, Culture, Sports, Science, and Technology of Japan.

References

[1] Y. Echelard, et al., Sonic hedgehog, a member of a family of putative signaling molecules, is implicated in the regulation of CNS polarity, Cell 75 (1993) 1417–1430.
[2] S. Krauss, J.P. Concordet, P.W. Ingham, A functionally conserved homolog of the Drosophila segment polarity gene hh is expressed in tissues with polarizing activity in zebrafish embryos, Cell 75 (1993) 1431–1444.
[3] R. Haraguchi, et al., Unique functions of Sonic hedgehog signaling during external genitalia development, Development 128 (2001) 4241–4250.
[4] E. Koyama, et al., Polarizing activity, Sonic hedgehog, and tooth development in embryonic and postnatal mouse, Dev. Dyn. 206 (1996) 59–72.
[5] J.W. Saunders, M.T. Gasseling, Ectodermal–mesenchymal interactions in the origin of limb symmetry, in: R. Fleischmajor, R.E. Billingham (Eds.), Epithelial–Mesenchymal Interactions, Williams & Wilkins, Baltimore, 1968, pp. 78–97.
[6] C. Tickle, D. Summerbell, L. Wolpert, Positional signalling and specification of digits in chick limb morphogenesis, Nature 254 (1975) 199–202.
[7] R.D. Riddle, R.L. Johnson, E. Laufer, C. Tabin, Sonic Hedgehog mediates the polarizing activity of ZPA, Cell 75 (1993) 1401–1416.
[8] D.T. Chang, et al., Products, genetic linkage and limb patterning activity of a murine hedgehog gene, Development 120 (1994) 3339–3353.
[9] E. Laufer, C.E. Nelson, R.L. Johnson, B.A. Morgan, C. Tabin, Sonic hedgehog and Fgf-4 act through a signaling cascade and feedback loop to integrate growth and patterning of the developing limb bud, Cell 79 (1994) 993–1003.
[10] N. Niswander, S. Jeffrey, G.R. Martin, C. Tickle, A positive feedback loop coordinates growth and patterning in the vertebrate limb, Nature 371 (1994) 609–612.
[11] A. Lopez-Martineze, et al., Limb-patterning activity and restricted posterior localization of the amino-terminal product of Sonic hedgehog cleavage, Curr. Biol. 5 (1995) 791–796.

[12] B. Wang, J.F. Fallon, P.A. Beachy, Hedgehog-regulated processing of Gli3 produces an anterior/posterior repressor gradient in the developing vertebrate limb, Cell 100 (2000) 423–434.
[13] Y. Litingtung, R.D. Dahn, Y. Li, J.F. Fallon, C. Chiang, Shh and Gli3 are dispensable for limb skeleton formation but regulate digit number and identity, Nature 418 (2002) 979–983.
[14] P. te Welscher, et al., Progression of vertebrate limb development through SHH-mediated counteraction of GLI3, Science 298 (2002) 827–830.
[15] M. Persson, et al., Dorsal–ventral patterning of the spinal cord requires Gli3 transcriptional repressor activity, Genes Dev. 16 (2002) 2865–2878.
[16] D.C. Chan, E. Laufer, C. Tabin, P. Leder, Polydactylous limbs in Strong's Luxoid mice result from ectopic polarizing activity, Development 121 (1995) 1971–1978.
[17] H. Masuya, T. Sagai, S. Wakana, K. Moriwaki, T. Shiroishi, A duplicated zone of polarizing activity (ZPA) in polydactylous mouse mutants, Genes Dev. 9 (1995) 1645–1653.
[18] H. Masuya, T. Sagai, K. Moriwaki, T. Shiroishi, Multigenic control of the localization of the zone of polarizing activity in limb morphogenesis in the mouse, Dev. Biol. 182 (1997) 42–51.
[19] S. Qu, et al., Mutations in mouse Aristaless-like4 cause Strong's luxoid polydactyly, Development 125 (1998) 2711–2721.
[20] M. Takahashi, et al., The role of Alx-4 in the establishment of anteroposterior polarity during vertebrate limb development, Development 125 (1998) 4417–4425.
[21] L. Lettice, J. Hecksher-Sorensen, R.E. Hill, The dominant hemimelia mutation uncouples epithelial–mesenchymal interactions and disrupts anterior mesenchyme formation in mouse hindlimbs, Development 126 (1999) 4729–4736.
[22] Y. Yada, S. Makino, S. Chigusa-Ishiwa, T. Shiroishi, The mouse polydactylous mutation, luxate (lx), causes anterior shift of the anteroposterior border in the developing hindlimb bud, Int. J. Dev. Biol. 46 (2002) 975–982.
[23] J. Sharpe, et al., Identification of sonic hedgehog as a candidate gene responsible for the polydactylous mouse mutant Sasquatch, Curr. Biol. 9 (1999) 97–100.
[24] L.A. Lettice, et al., Disruption of a long-range cis-acting regulator for Shh causes preaxial polydactyly, Proc. Natl. Acad. Sci. U.S.A. 99 (2002) 7548–7553.
[25] L.A. Lettice, et al., A long-range Shh enhancer regulates expression in the developing limb and fin and is associated with preaxial polydactyly, Hum. Mol. Genet. 12 (2003) 1725–1735.
[26] T. Sagai, et al., Phylogenetic conservation of a limb-specific, cis-acting regulator of Sonic hedgehog (Shh), Mamm. Genome 15 (2004) 23–34.
[27] D.J. Epstein, A.P. McMahon, A.L. Joyner, Regionalization of Sonic hedgehog transcription along the anteroposterior axis of the mouse central nervous system is regulated by Hnf3-dependent and-independent mechanisms, Development 126 (1999) 281–292.
[28] T. Sagai, M. Hosoya, Y. Mizushina, M. Tamura, T. Shiroishi, Elimination of a long-range cis-regulatory module causes complete loss of limb-specific Shh expression and truncation of the mouse limb, Development 132 (2005) 797–803.
[29] M.A. Ros, et al., The chick oligozeugodactyly (ozd) mutant lacks sonic hedgehog function in the limb, Development 130 (2003) 527–537.
[30] S.A. Maas, J.F. Fallon, Isolation of the chicken Lmbr1 coding sequence and characterization of its role during chick limb development, Dev. Dyn. 229 (2004) 520–528.
[31] S.A. Maas, J.F. Fallon, Single base pair change in the long-range Sonic hedgehog limb-specific enhancer is a genetic basis for preaxial polydactyly, Dev. Dyn. 232 (2005) 345–348.
[32] S. Hitotsumachi, D.A. Carpenter, W.L. Russell, Dose-repetition increases the mutagenic effectiveness of N-ethyl-N-nitrosourea in mouse spermatogonia, Proc. Natl. Acad. Sci. U.S.A. 82 (1985) 6619–66121.
[33] L.B. Russell, J.W. Bangham, K.F. Stelzner, P.R. Hunsicker, High frequency of mosaic mutants produced by N-ethyl-N-nitrosourea exposure of mouse zygotes, Proc. Natl. Acad. Sci. U.S.A. 85 (1988) 9167–9170.
[34] P.M. Nolan, D. Kapfhamer, M. Bucan, Random mutagenesis screen for dominant behavioral mutations in mice, Methods 13 (1997) 379–395.
[35] E.L. Coghill, et al., A gene-driven approach to the identification of ENU mutants in the mouse, Nat. Genet. 30 (2002) 255–256.
[36] Y. Sakuraba, et al., Molecular characterization of ENU mouse mutagenesis and archives, Biochem. Biophys. Res. Commun. 336 (2005) 609–616.
[37] E.M. Rinchik, D.A. Carpenter, N-Ethyl-N-nitrosourea mutagenesis of a 6-to 11-cM subregion of the Fah-Hbb interval of mouse chromosome 7: completed testing of 4557 gametes and deletion mapping and complementation analysis of 31 mutations, Genetics 152 (1999) 373–383.
[38] P.M. Nolan, et al., A systematic, genome-wide, phenotype-driven mutagenesis programme for gene function studies in the mouse, Nat. Genet. 25 (2000) 440–443.
[39] M.H. Hrabe de Angelis, et al., Genome-wide, large-scale production of mutant mice by ENU mutagenesis, Nat. Genet. 25 (2000) 444–447.
[40] B.T. Kile, et al., Functional genetic analysis of mouse chromosome 11, Nature 425 (2003) 81–86.
[41] H. Masuya, et al., Development and implementation of a database system to manage a large-scale mouse ENU-mutagenesis program, Mamm. Genome 15 (2004) 404–411.
[42] D. Goldowitz, et al., Large-scale mutagenesis of the mouse to understand the genetic bases of nervous system structure and function, Mol. Brain Res. 132 (2004) 105–115.
[43] L. Wilson, et al., Random mutagenesis of proximal mouse chromosome 5 uncovers predominantly embryonic lethal mutations, Genome Res. 15 (2005) 1095–1105.
[44] H. Masuya, et al., Implementation of the modified-SHIRPA protocol for screening of dominant phenotypes in a large-scale ENU mutagenesis program, Mamm. Genome 16 (2005) 829–837.
[45] J.L. Vivian, Y. Chen, D. Yee, E. Schneider, T. Magnuson, An allelic series of mutations in Smad2 and Smad4 identified in a genotype-based screen of N-ethyl-N-nitrosourea-mutagenized mouse embryonic stem cells, Proc. Natl. Acad. Sci. U.S.A. 99 (2002) 15542–15547.
[46] M. Inoue, et al., A series of maturity onset diabetes of the young, type 2 (MODY2) mouse models generated by a large-scale ENU mutagenesis program, Hum. Mol. Genet. 13 (2004) 1147–1157.
[47] M.M. Quwailid, et al., A gene-driven ENU-based approach to generating an allelic series in any gene, Mamm. Genome 15 (2004) 585–591.
[48] H. Masuya, et al., Enamelin (Enam) is essential for amelogenesis: ENU-induced mouse mutants as models for different clinical subtypes of human amelogenesis imperfecta (AI), Hum. Mol. Genet. 14 (2005) 575–583.
[49] J. Graw, et al., Three novel Pax6 alleles in the mouse leading to the same small-eye phenotype caused by different consequences at target promoters, Invest. Ophthalmol. Visual Sci. 46 (2005) 4671–4683.
[50] Q. Li, Z. Liu, H. Monroe, C.T. Culiat, Integrated platform for detection of DNA sequence variants using capillary array electrophoresis, Electrophoresis 23 (2002) 1499–1511.
[51] Q. Gao, E.S. Yeung, High-throughput detection of unknown mutations by using multiplexed capillary electrophoresis with poly(vinylpyrrolidone) solution, Anal. Chem. 72 (2000) 2499–2506.
[52] M. Tsugane, M. Yasuda, Dermatoglyphics on volar skin of mice: the normal pattern, Anat. Rec. 242 (1995) 225–232.
[53] N. Wanek, K. Muneoka, G. Holler-Dinsmore, R. Burton, S.V. Bryant, A staging system for mouse limb development, J. Exp. Zool. 249 (1989) 41–49.
[54] P. Patel, B.B. Nankova, E.F. LaGamma, Nicotinic induction of preproenkephalin and tyrosine hydroxylase gene expression in butyrate-differentiated rat PC12 cells: a model for adaptation to gut-derived environmental signals, Pediatr. Res. 53 (2003) 113–118.
[55] Y. Xie, M. Li, Y. Wang, P.H. Hofschneider, L. Weiss, Site-specific mutation of the hepatitis B virus enhancer II B1 element: effect on virus transcription and replication, J. Gen. Virol. 82 (2001) 531–535.
[56] L.D. Norquay, et al., A member of the nuclear factor-1 family is involved in the pituitary repression of the human placental growth hormone genes, Biochem. J. 354 (2001) 387–395.
[57] E.J. Chesler, et al., Complex trait analysis of gene expression uncovers polygenic and pleiotropic networks that modulate nervous system function, Nat. Genet. 37 (2005) 233–242.
[58] R.A. Radcliffe, M.J. Lee, R.W. Williams, Prediction of cis-QTLs in a pair

of inbred mouse strains with the use of expression and haplotype data from public databases, Mamm. Genome 17 (2006) 629–642.
[59] K.R. Shockley, G.A. Churchill, Gene expression analysis of mouse chromosome substitution strains, Mamm. Genome 17 (2006) 598–614.
[60] V.N. Kristensen, et al., Genetic variation in putative regulatory loci controlling gene expression in breast cancer, Proc. Natl. Acad. Sci. U.S.A. 103 (2006) 7735–7740.
[61] S. Mahr, et al., Cis-and trans-acting gene regulation is associated with osteoarthritis, Am. J. Hum. Genet. 78 (2006) 793–803.
[62] M. Fernandez-Teran, et al., Role of dHAND in the anterior–posterior polarization of the limb bud: implications for the Sonic hedgehog pathway, Development 127 (2000) 2133–2142.
[63] J. Charite, D.G. McFadden, E.N. Olson, The bHLH transcription factor dHAND controls Sonic hedgehog expression and establishment of the zone of polarizing activity during limb development, Development 127 (2000) 2461–2470.
[64] M. Fernandez-Teran, M.E. Piedra, J.C. Rodriguez-Rey, A. Talamillo, M.A. Ros, Expression and regulation of eHAND during limb development, Dev. Dyn. 226 (2003) 690–701.
[65] C.S. Shashikant, et al., Regulation of Hoxc-8 during mouse embryonic development: identification and characterization of critical elements involved in early neural tube expression, Development 121 (1995) 4339–4347.
[66] R. Kothary Clapoff, et al., Inducible expression of an hsp68-lacZ hybrid gene in transgenic mice, Development 105 (1989) 707–714.